GDCh Research Article Angewandte International Edition Chemie www.angewandte.org

Check for updates

How to cite: *Angew. Chem. Int. Ed.* **2025**, e202512575
doi.org/10.1002/anie.202512575

Polymer Chemistry Hot Paper

Driving Multi-Step Regioselectivity in On-Surface Polymer Synthesis by Molecular Coverage

Kalyan Biswas[+], Alba García-Frutos[+], Berta Álvarez, Marco Lozano, Ana Barragán, Jesús Janeiro, Jesús Bello-García, Diego Soler-Polo, Koen Lauwaet, José M. Gallego, Dolores Pérez, Rodolfo Miranda, José I. Urgel, Pavel Jelínek,* Diego Peña,* and David Écija**

Abstract: On-surface synthesis has revolutionized the design of low-dimensional organic nanomaterials, introducing unprecedented families of compounds while offering precise control over their structural and functional properties. A critical challenge in this field is achieving regioselective control over covalent bond formation, which is essential for tailoring polymerization processes. Here, we demonstrate a novel approach toward regioselective polymerization on Au(111) using a dicyclopentaanthracene precursor, an acene derivative that comprise two terminal indene moieties. Through a combination of scanning tunneling microscopy, non-contact atomic force microscopy, and density functional theory calculations, we reveal a molecular coverage-dependent regioselective homocoupling mechanism. At low coverage, one-dimensional polymers formed via indenyl couplings in *anti*-configuration dominate, involving both five-membered rings of the precursor. Increasing the coverage to half a monolayer shifts the regioselectivity, yielding a quasi-1D staircase polymer through indenyl couplings that engage only one five-membered ring of each precursor. At higher coverages, a two-dimensional porous network emerges, driven by the activation of the four benzylic positions of the molecular precursor. Our findings highlight the ability to steer regioselectivity and, consequently, polymer dimensionality by controlling molecular coverage, significantly advancing the fields of on-surface synthesis and polymer science.

Introduction

On-surface synthesis has emerged over the past two decades as a distinct discipline in chemistry, physics and material science enabling the design of low-dimensional materials at interfaces while allowing the study of their intrinsic physicochemical properties with remarkable spatial resolution.[1–3] A key aspect of this field is the ability to tailor specific covalent products by identifying and controlling the parameters necessary to synthesize the desired organic nanomaterials.[4–6]

Regioselectivity is a fundamental concept in chemistry that dictates the preferential formation of bonds at specific positions within a molecule during a chemical reaction.[7,8] This control is especially crucial in polymerization processes, where the precise arrangement of monomers determines the structural and functional properties of the resulting polymer.

[*] Dr. K. Biswas[+], A. García-Frutos[+], Dr. A. Barragán, Dr. K. Lauwaet, Prof. R. Miranda, Dr. J. I. Urgel, Prof. D. Écija
IMDEA Nanoscience, Campus de Cantoblanco, C/ Faraday 9, Madrid 28049, Spain
E-mail: jose-ignacio.urgel@imdea.org
david.ecija@imdea.org

B. Álvarez, J. Janeiro, Dr. J. Bello-García, Prof. D. Pérez, Prof. D. Peña
Centro de Investigación en Química Biolóxica e Materiais Moleculares (CiQUS) and Departamento de Química Orgánica, Universidade de Santiago de Compostela, E-15782, Santiago de Compostela, Spain
E-mail: diego.pena@usc.es

M. Lozano, D. Soler-Polo, Prof. P. Jelínek
Institute of Physics of the Czech Academy of Science, Praha CZ-16253, Czech Republic
E-mail: jelinekp@fzu.cz

M. Lozano, Prof. P. Jelínek
Regional Centre of Advanced Technologies and Materials, Palacký University Olomouc, Olomouc 771 46, Czech Republic

Dr. J. M. Gallego
Instituto de Ciencia de Materiales de Madrid, CSIC, Cantoblanco, Madrid 28049, Spain

Prof. R. Miranda
Departamento de Física de la Materia Condensada, Universidad Autónoma de Madrid, Madrid 28049, Spain

Dr. J. I. Urgel, Prof. D. Écija
Unidad de Nanomateriales Avanzados, IMDEA Nanoscience, Unidad asociada al CSIC por el ICMM, Campus de Cantoblanco, C/ Faraday 9, Madrid 28049, Spain

Prof. D. Peña
Oportunius, Galician Innovation Agency (GAIN), Santiago de Compostela 15702, Spain

[+] Both authors equally contributed to this work.

Additional supporting information can be found online in the Supporting Information section

© 2025 The Author(s). Angewandte Chemie International Edition published by Wiley-VCH GmbH. This is an open access article under the terms of the Creative Commons Attribution-NonCommercial-NoDerivs License, which permits use and distribution in any medium, provided the original work is properly cited, the use is non-commercial and no modifications or adaptations are made.

© 2025 The Author(s). Angewandte Chemie International Edition published by Wiley-VCH GmbH

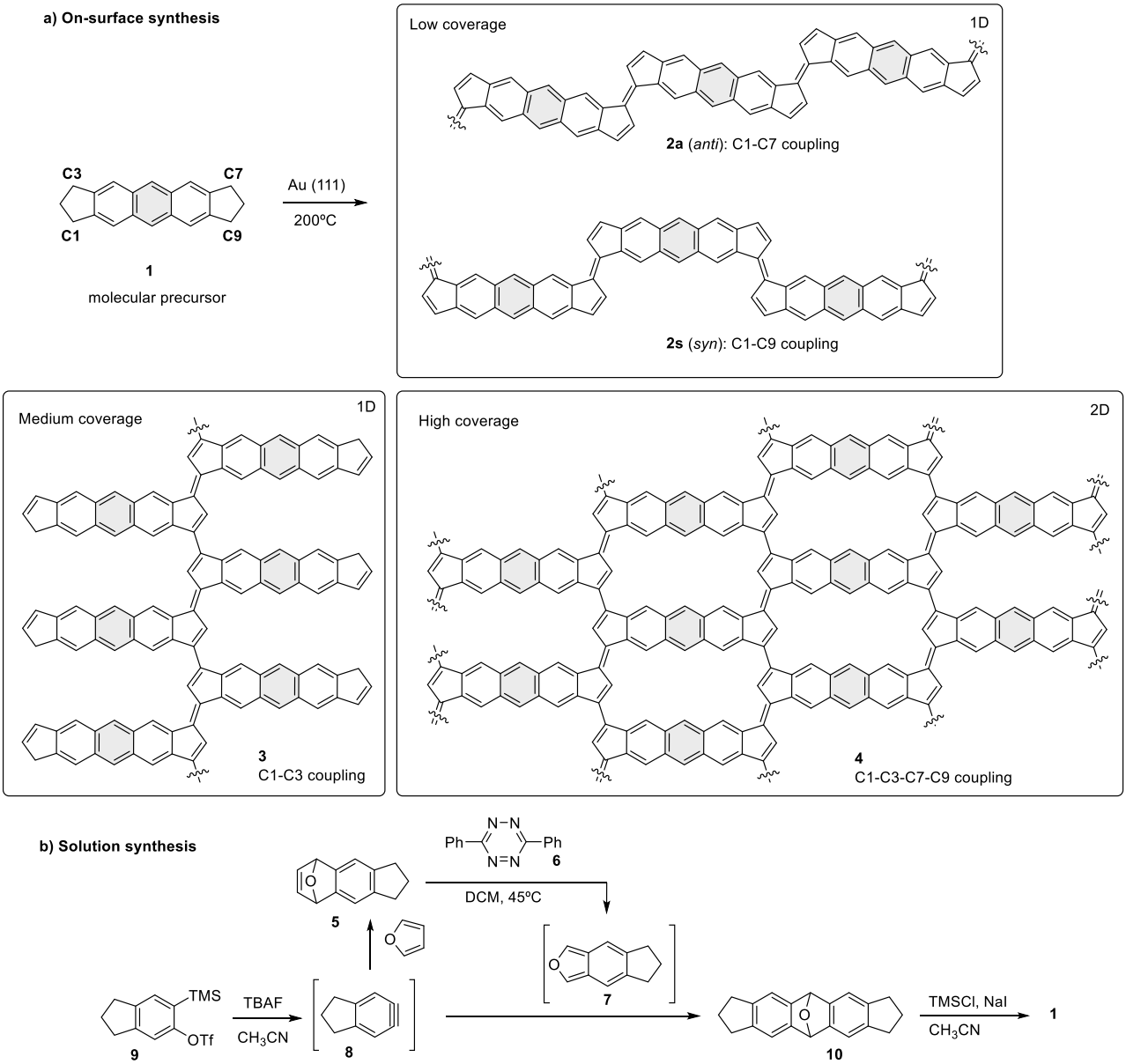

Scheme 1. Molecular coverage as a reaction parameter to steer regioselective homocoupling mechanism. a) On-surface synthesis of **1** to 1D polymers with *anti*- and *syn*-linking (**2a** and **2s**), 1D staircase polymers (**3**), and 2D networks (**4**) driven by molecular coverage and formed via activation at carbons at different sites of the precursors upon deposition on Au(111) at room temperature and subsequent annealing to 200 °C. b) Solution-phase synthesis of the molecular precursor **1**.

In the realm of on-surface synthesis, various parameters have been explored to tailor reaction products, including the nature,[9] structure,[10,11] and temperature of the substrate[12–14] molecular coverage;[15] and precursor stoichiometry.[16] However, achieving regioselectivity in the polymerization of organic nanomaterials through an external parameter on surfaces has remained elusive.

Recently, we discovered a regio- and stereo-selective coupling of indenyl moieties that affords the formation of one-dimensional polymers on Au(111) by exploiting molecular precursors equipped with a terminal five-membered carbon ring.[17] Building on this reaction, we have synthesized dicyclopentaanthracene **1**, bearing two terminal five-membered rings, in order to explore the possible formation of 2D porous nanostructures by indenyl coupling on Au(111). Based on our previous work,[17] the four benzylic positions of compound **1** (i.e., C1, C3, C7, and C9) could be involved in an indenyl coupling (Scheme 1a). Our comprehensive scanning probe microscopy study, combining scanning tunneling microscopy (STM), scanning tunneling spectroscopy (STS), and non-contact atomic force microscopy (nc-AFM), complemented by density functional theory (DFT) calculations, illustrates that when these precursors are deposited on the metal substrate and annealed to 200 °C, a multistep regioselective homocoupling reaction is observed, being triggered by molecular coverage. At very low coverage, the predominant formation (48 ± 2%) of the one-dimensional (1D) polymer

© 2025 The Author(s). Angewandte Chemie International Edition published by Wiley-VCH GmbH

15213773, 0, Downloaded from https://onlinelibrary.wiley.com/doi/10.1002/anie.202512575 by Universidad Autonoma De Madrid, Wiley Online Library on [30/10/2025]. See the Terms and Conditions (https://onlinelibrary.wiley.com/terms-and-conditions) on Wiley Online Library for rules of use; OA articles are governed by the applicable Creative Commons License

2a with *anti*-configuration is observed (C1–C7 coupling), which coexists with minority sections (24 ± 2%) of the *syn*-polymer **2s** (C1-C9 coupling). Increasing the coverage to half a monolayer drastically alters such scenario, since now a quasi-1D staircase polymer **3** is achieved, arising from the regioselective coupling exclusively involving activation at carbons C1 and C3 of the precursors. Finally, at higher coverages, small patches of a two-dimensional (2D) porous network **4** are formed, based on the activation of all the benzylic carbon atoms.

Our results illustrate the potential to steer regioselectivity by molecular coverage at interfaces, enabling the design of polymers featuring distinct dimensionality, thus notably expanding the toolbox of on-surface synthesis and polymer science.

Results and Discussion

Inspired by our recent on-surface synthesis of acenoindenylidene polymers exploiting a regio- and stereo-selective indenyl coupling of acene derivatives,[17] we have designed 1,2,3,7,8,9-hexahydrodicyclopenta[*b*,*i*]anthracene (**1**) due to its potential to drive homocoupling from both termini at the metal interface. The synthesis of precursor **1** was achieved in the solution phase by means of aryne chemistry, as shown in Scheme 1b. Thus, treatment of compound **5**[18] with 3,6-di-2-pyridyl-1,2,4,5-tetrazine (**6**) afforded the highly reactive isobenzofuran **7**, which was reacted with aryne **8** (generated from **9** with tetrabutylammonium fluoride), leading to the formation of the epoxy derivative **10** by a Diels–Alder reaction. It should be mentioned that compound **5** was also obtained from triflate **9** by [4 + 2] cycloaddition of aryne **8** with furan. Finally, compound **10** was subjected to a deoxygenative aromatization protocol to afford the dicyclopentaanthracene **1**, which was employed for the on-surface experiments. Further synthesis and characterization details are provided in Figures S1–S3.

The deposition of a submonolayer coverage of **1** on an Au(111) held at room temperature resulted in the formation of a supramolecular assembly based on intact molecules stabilized by van der Waals interactions (cf. Figure S4).

Once the integrity of species **1** upon adsorption was confirmed, we proceeded to examine the influence of the molecular coverage on potential homocoupling reactions. Annealing at 200 °C a low coverage sample of **1** (0.16 ± 0.03 ML) on Au(111) affords the formation of 1D polymers with an *anti*-configuration (**2a**). These polymers feature regioselective homocoupling between adjacent monomers (48 ± 2% of frequency) involving carbons C1 and C7 of each species, thanks to dehydrogenation and subsequent carbon–carbon bond formation, as illustrated in Figure 1a,b by STM imaging. This initial step of dehydrogenation results in some isolated monomeric species, namely 1,7-dihydrodicyclopenta[*b*,*i*]anthracene, due to dehydrogenation at the C1 and C7 positions. The structural characterization and associated electronic properties of such monomers are presented in Figure S5. Residual homocoupling between carbons C1 and C9 of the species results in minor sections of the *syn*-polymer (**2s**, 24 ± 2%). Defective connections scale up to 23 ± 2% (see Table S1).

Importantly, high-resolution frequency shift nc-AFM images (Figure 1c,d) reveal that the monomers have lost the extra hydrogen atoms from each of the five-member units of the precursor, i.e., they have undergone a six-fold hydrogen cleavage. The quality of the nc-AFM images ratifies the structural identification of the monomers as dicycloanthracene-based moieties, which is further supported by nc-AFM simulations using the PP-AFM code[19] (Figure S6). Notably, the potential radical character of the polymers at the termini (Figure 1e) is quenched by either incomplete dehydrogenation of unlinked sites or, alternatively, if initially dehydrogenated, by passivation through residual atomic hydrogen, as depicted in Figure 1g.

Next, we characterized the electronic structure of polymer **2a** by STS at selected positions, revealing prominent features at −0.77 and 1.04 V (cf. Figure 1h). Experimental dI/dV mapping acquired at such resonances and comparison with theoretical dI/dV maps[19] obtained from DFT calculations[20] of the valence band maximum (VBM) and the conduction band minimum (CBM) of the polymer (cf. Figure 1i), allow us to establish a bandgap of 1.81 eV. In comparison, sections of polymer **2s** display a slightly higher bandgap of 2.01 eV (cf. Figure S7).

Increasing the molecular coverage of **1** to close to half a monolayer on pristine Au(111) (0.44 ± 0.06 ML) and further annealing at 200 °C results in a drastically different scenario. We observe the formation of long sections of 1D staircase polymers **3**, spanning the whole surface (cf. Figure 2a). High-resolution STM and nc-AFM frequency shift images (cf. Figure 2b–d) allows to unambiguously discern dicyclopentaanthracene-based moieties linked through carbon–carbon couplings. These arise from the regioselective activation of carbons C1 and C3 of the same five-membered ring of each precursor (50 ± 1% in frequency, see Table S1), in an analogous reaction as the one previously found by us for cyclopentaanthracene on Au(111).[17] Notably, a bright protrusion is observed by nc-AFM imaging at the termini of each monomer and assigned to an extra-hydrogenation of those carbon positions, which allows us to propose a dominant resonant form of the polymer expressing one Clar sextet per monomer (cf. Figures 2e and S8). Thus, while the system displays an intrinsic tendency toward open-shell character, the residual atomic hydrogen atoms in the chamber passivate any potential radicalism (Figure S6). Comparing polymers **2a** and **3**, it is worthmentioning that the regioselectivity has has changed from involving carbons C1 and C7 from different five-membered rings to carbons C1 and C3 of the same five-membered moiety, as depicted in Scheme 1. We tentatively attribute such a phenomenon to the increase in the molecular coverage. In the first scenario, molecules are sparsely distributed across the surface, and they prefer to interact through carbons C1 and C7. However, for a certain coverage (above half a monolayer), some areas form minute supramolecular assemblies, even at high temperature, promoting covalent nucleation sites and the regioselectivity via carbons C1 and C3. This behavior is illustrated in Figure S4 by probing a supramolecular

© 2025 The Author(s). Angewandte Chemie International Edition published by Wiley-VCH GmbH

15213773, 0, Downloaded from https://onlinelibrary.wiley.com/doi/10.1002/anie.202512575 by Universidad Autonoma De Madrid, Wiley Online Library on [30/10/2025]. See the Terms and Conditions (https://onlinelibrary.wiley.com/terms-and-conditions) on Wiley Online Library for rules of use; OA articles are governed by the applicable Creative Commons License

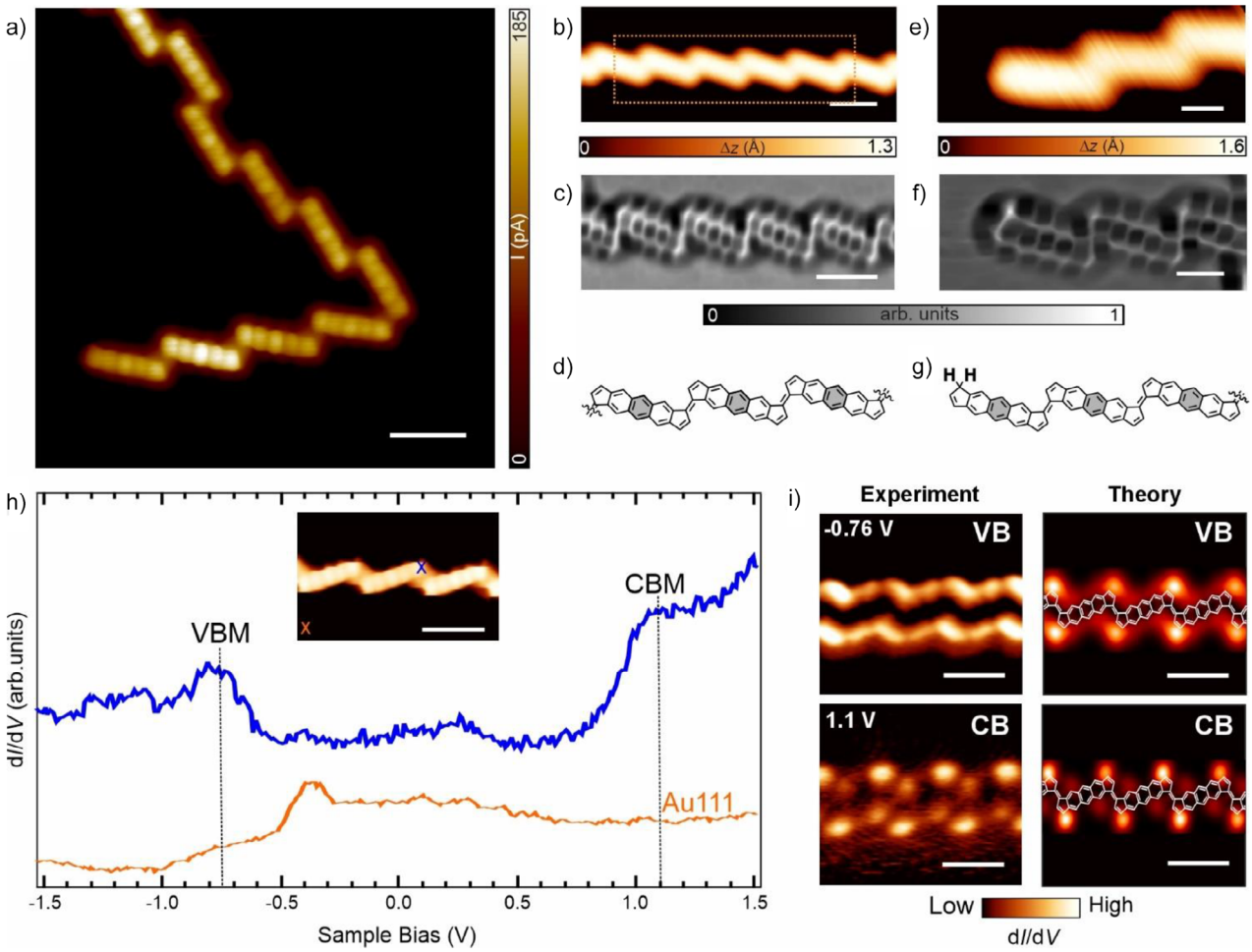

Figure 1. Low coverage: Structural and electronic characterization of 1D polymer with *anti-* and *syn*-connections on Au(111). a) Constant-height high-resolution overview STM image acquired with a CO-functionalized tip of an Au111) surface after the deposition of a low coverage (0.16 ± 0.03 ML) of precursor **1** and subsequent annealing to 200 °C. V = 5 mV, I = 50 pA, Z_{offset} = 100 pm, scale bar = 1 nm. b) and e) Constant-current high-resolution STM images of polymers **2a** without and with a terminus, respectively. (b) V = 100 mV, I = 10 pA and (e) V = 0.5 V, I = 50 pA, c) and f) Laplace-filtered constant-height frequency-shift nc-AFM images of a selected segment (marked with orange rectangle box) of (b) and (e) acquired with a CO-functionalized tip V = 5 mV, 50 pA, Z_{offset} = 150 pm (b) and 200 pm (e), scale bar (b, c) = 1 nm and (e, f) = 0.5 nm. d) and g) Chemical sketch of the resulting polymer shown in (c, f). h) d*I*/d*V* spectra with two pronounced peaks of **2a** polymers acquired at the positions indicated by the blue-colored cross inset image. Reference spectra taken on the bare Au(111) surface is depicted in orange, and the acquisition position is marked with an orange cross in the inset image. Open feedback parameters for d*I*/d*V* spectra: V = −1.5 V, I = 100 pA, V_{rms} = 20 mV. Scanning parameter of inset image V = 5 mV, I = 30 pA, scale bar = 1 nm. i) Constant current d*I*/d*V* maps acquired at the approximate energies of the VB and CB (left) with the corresponding simulated maps (right). d*I*/d*V* parameters: VB (V = −0.76 V, I = 250 pA) and CB (V = 1.1 V, I = 250 pA), with V_{rms} = 20 mV.

assembly of **1** on Au(111) held at rt, in which the interacting motifs favor the subsequent formation of polymer **3** upon annealing.

The characterization of the electronic structure of an oligomer of **3** reveals resonances at −0.19 and 0.19 eV, respectively. d*I*/d*V* mapping at such energy values displays the onsets of the VB and CB, respectively, which match nicely with the theoretical modelling of a free-standing polymer, thus ratifying our rationalization and revealing a bandgap of 0.38 eV.

Notably, at such medium coverage, we concomitantly observed the formation of very small 2D covalent porous networks (**4,** 25 ± 1% in frequency; see Table S1). Increasing the coverage of **1** close to the monolayer (0.94 ± 0.05 ML) followed by annealing at 200 °C promotes higher lateral regioselective reactions, affording the synthesis of numerous small 2D covalent porous networks (**4**, cf. Figure 3a–c). In such nanoarchitectures, carbons C1, C3, C7, and C9 of each precursor have been activated for the regioselective homocoupling through single carbon-carbon bonds in a staircase fashion (73 ± 2% in frequency; see Table S1). Again, the reason for such architectonics is presumably related to local supramolecular assembly at high coverages that initiates as a seed the covalent reaction, driving the most favorable reaction sides. Thanks to the nc-AFM frequency shift high-resolution images with a CO functionalized tip, the dicyclopentaanthracene-like moiety is discerned, and importantly, the rules for determining the dominant resonant form can be established (cf. Figure 3d). In principle, a Clar sextet per monomer could be possible to drawn, which would imply that each five-member ring not connected to its

© 2025 The Author(s). Angewandte Chemie International Edition published by Wiley-VCH GmbH

15213773, 0, Downloaded from https://onlinelibrary.wiley.com/doi/10.1002/anie.202512575 by Universidad Autonoma De Madrid, Wiley Online Library on [30/10/2025]. See the Terms and Conditions (https://onlinelibrary.wiley.com/terms-and-conditions) on Wiley Online Library for rules of use; OA articles are governed by the applicable Creative Commons License

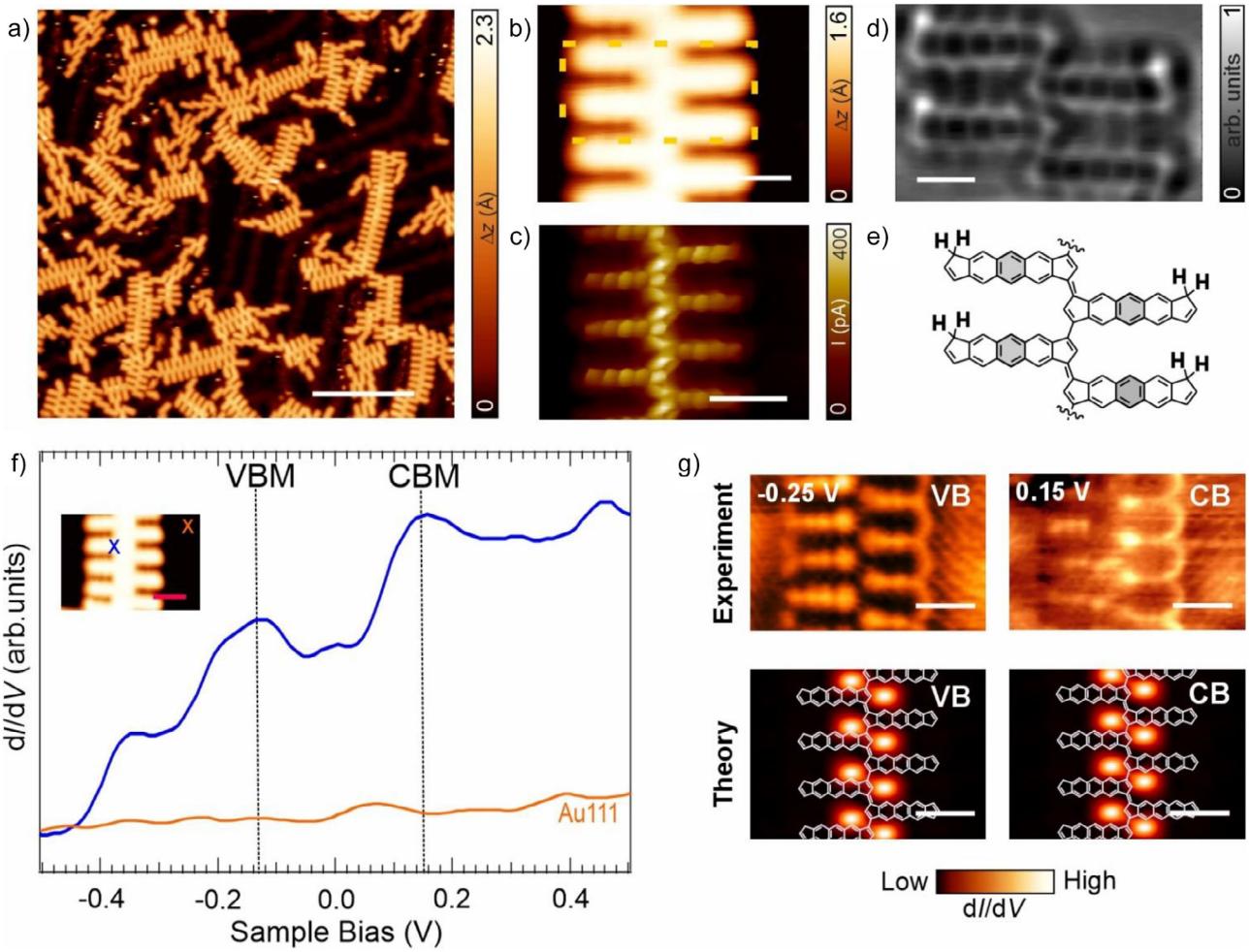

Figure 2. Medium coverage: Structural and electronic characterization of 1D staircase polymers **3**. a) Overview STM topography image with 0.44 ± 0.06 ML coverage showing the formation of 1D staircase (polymer **3**) after deposition of **1** and subsequent annealing at 200 °C, V = −100 mV, I = 100 pA, scale bar = 10 nm. b) Magnified constant current STM image of a 1D staircase polymer (**3**), V = 5 mV, I = 10 pA, scale bar = 0.5 nm, and c) high-resolution constant-height STM image of the same segment, V = 5 mV, I = 50 pA, Z_{offset} = 0 pm, scale bar = 1 nm. d) Constant-height Laplace-filtered nc-AFM image from selected area (yellow box) of (b), V = 5 mV, I = 50 pA, Z_{offset} = 200 pm, scale bar = 0.5 nm. e) Corresponding chemical sketch of the nc-AFM image in (d). f) Experimental determination of bandgap for **3** with STS acquired at the positions depicted by colored cross in inset image 4 × 4 nm^2, scale bar = 1 nm and orange curve on Au(111). Open feedback parameters for d*I*/d*V* spectra: V = −1.5 V, I = 100 pA, V_{rms} = 20 mV. g) Experimental d*I*/d*V* map of the VB and CB at constant current (left panel) and with the corresponding simulated maps (right panel). d*I*/d*V* map parameters: VB (V = −0.25 V, I = 250 pA) and CB (V = 0.15 V, I = 250 pA), with V_{rms} = 20 mV. Scale bar = 1 nm.

neighbors through single C-C bonds would present a radical, or, alternatively, be passivated by residual atomic hydrogen, as is the case (cf. Figure 3e).

Concerning the electronic structure, STS over selected positions of a small patch reveals resonances at −0.5 and 0.25 V. In a second step, such resonances are spatially probed by d*I*/d*V* mapping, matching nicely with the theoretical modelling, and thus allowing us to set the onsets of the VB and CB, establishing an overall bandgap of 0.75 eV.

Conclusion

In conclusion, our study demonstrates a strategy for tuning regioselective polymerization on Au(111) by molecular coverage as a control parameter. We demonstrate that the activation sites of dicyclopentaanthracene precursors systematically shift with molecular coverage. In a first step, annealing a low coverage of the precursor on Au(111) at 200 °C resulted in 1D *anti*-polymers based on the activation of carbons C1 and C7 of the precursor through dehydrogenation and homocoupling of adjacent species. Repeating the same procedure with half a monolayer of coverage gives rise to 1D staircase polymers new opportunities through the activation of carbons C1 and C3 of each species, thus illustrating the regioselective control of an on-surface reaction by molecular coverage. A final increase of molecular coverage over 0.9 ML and annealing to 200 °C triggers not only a distinct regioselectivity, this time based on the cascade activation of carbons C1, C3, C7, and C9, but also changes the dimensionality of the system, now driving to small patches of a 2D covalent porous network.

Our study introduces new opportunities to tailor on-surface chemical reactions at interfaces, propelling fascinating

© 2025 The Author(s). Angewandte Chemie International Edition published by Wiley-VCH GmbH

15213773, 0, Downloaded from https://onlinelibrary.wiley.com/doi/10.1002/anie.202512575 by Universidad Autonoma De Madrid, Wiley Online Library on [30/10/2025]. See the Terms and Conditions (https://onlinelibrary.wiley.com/terms-and-conditions) on Wiley Online Library for rules of use; OA articles are governed by the applicable Creative Commons License

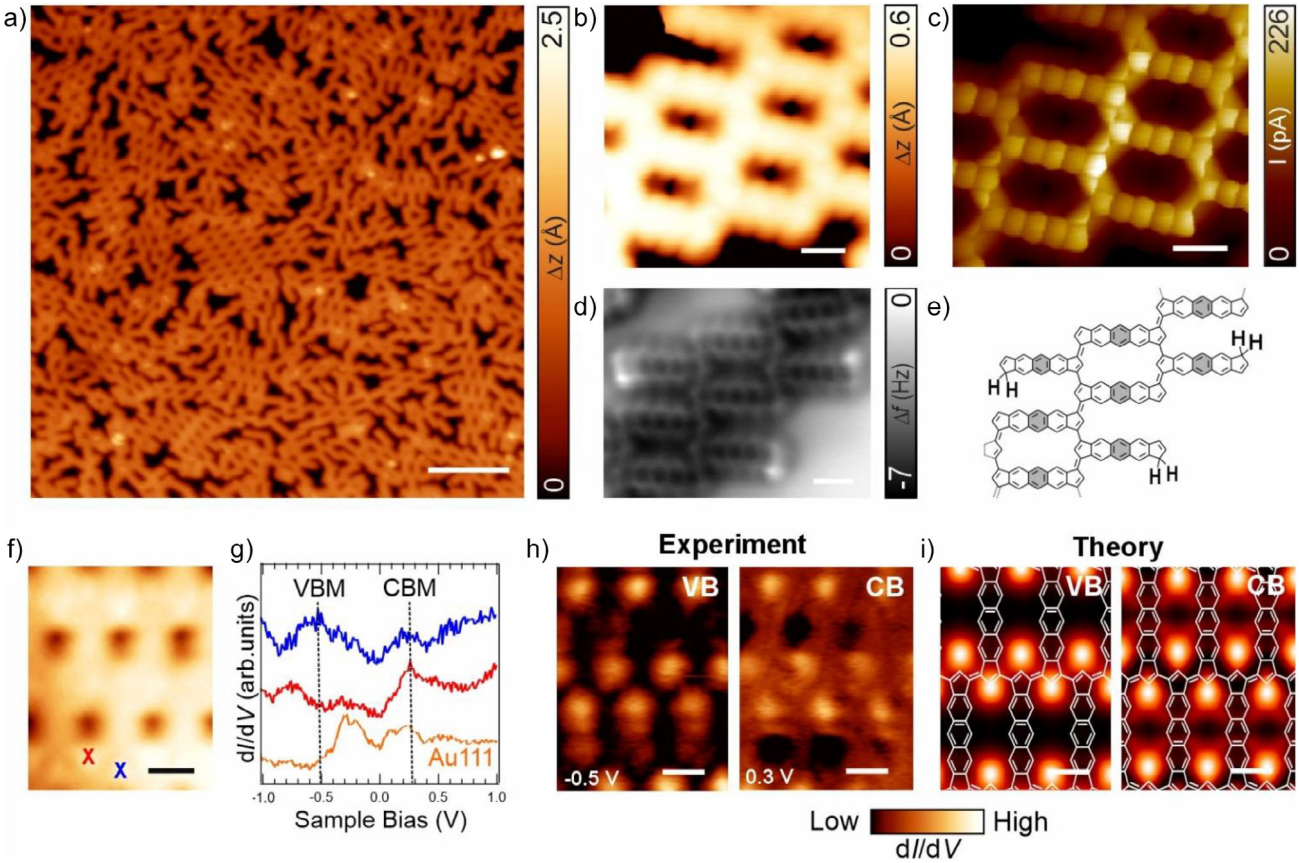

Figure 3. High coverage: Structural and electronic characterization of 2D covalent networks **4** on Au(111). a) An overview STM topography image displaying 0.94 ± 0.05 ML coverage illustrates the formation of small 2D patches (**4**) following the deposition of **1** and subsequent annealing at 200 °C (V = 0.5 V, I = 50 pA, scale bar = 5 nm). b) A zoom-in constant-current STM image highlights a segment of (**4**), while c) presents a high-resolution constant-height STM image of the same segment acquired with a CO-functionalized tip. Scanning parameters (b) V = 5 mV, I = 20 pA, c) V = 5 mV, I = 50 pA, Z_{offset} = 160 pm, scale bar (b, c) = 0.5 nm). d) A constant-height nc-AFM image of (**4**), V = 5 mV, I = 20 pA, Z_{offset} = 160 pm, scale bar = 0.5 nm. e) The corresponding chemical sketch represents the nc-AFM image shown in d). f) High-resolution STM topography image of a small patch of (**4**), V = −0.5 V, I = 250 pA, scale bar = 0.5 nm. g) Experimental d*I*/d*V* spectra on a 2D network at selected points indicated by the colored crosses in (f). h) Experimental constant-current d*I*/d*V* map of VB and CB, d*I*/d*V* map parameters: VB (V = −0.5 V, I = 250 pA) and CB (V = 0.3 V, I = 250 pA), with V_{rms} = 20 mV. i) corresponding simulated maps.

prospects for controlling site-specific reactions to drive the expression of polymeric architectures of increasing dimensionality and complexity.

Acknowledgements

This project has received funding from MCIN/AEI/10.13039/501100011033 through grants PID2019-108532GB-I00, PID2022-139933NB-I00, PID2022-140845OB-C62, and PID2023-152793NA-I00. The authors acknowledge the support from ERC SyG MolDAM (951519), and the "(MAD2D-CM)-IMDEA-Nanociencia" project funded by Comunidad de Madrid, by the Recovery, Transformation and Resilience Plan, and by NextGenerationEU from the European Union. The authors thank Comunidad de Madrid through Programa de Actividades de I+D (TEC-2024/TEC-459, SYNMOLMAT-CM). The authors appreciate support from the European Regional Development Fund of the European Union (EU) and from Xunta de Galicia (Centro de Investigación de Galicia accreditation 2019–2022, ED431G 2019/03). A.B. acknowledges financial support from Juan de la Cierva program (FJC2021-046524-I). J.I.U. acknowledges the funding from MCIU for the Ramón y Cajal (RYC2022-037352). P.J. and M.L. appreciate financial support from the CzechNanoLab Research Infrastructure supported by MEYS CR (LM2018110) and GACR 23–05486S.

Conflict of Interests

The authors declare no conflict of interest.

Data Availability Statement

The data that support the findings of this study are available from the corresponding author upon reasonable request.

© 2025 The Author(s). Angewandte Chemie International Edition published by Wiley-VCH GmbH

15213773, 0, Downloaded from https://onlinelibrary.wiley.com/doi/10.1002/anie.202512575 by Universidad Autonoma De Madrid, Wiley Online Library on [30/10/2025]. See the Terms and Conditions (https://onlinelibrary.wiley.com/terms-and-conditions) on Wiley Online Library for rules of use; OA articles are governed by the applicable Creative Commons License

Keywords: On-surface synthesis · Polymer science · Regioselectivity · Scanning probe microscopy

[1] L. Talirz, P. Ruffieux, R. Fasel, *Adv. Mater.* **2016**, *28*, 6222–6231. https://doi.org/10.1002/adma.201505738.
[2] Q. Sun, R. Zhang, J. Qiu, R. Liu, W. Xu, *Adv. Mater.* **2018**, *30*, 1705630. https://doi.org/10.1002/adma.201705630.
[3] Z. Chen, A. Narita, K. Müllen, *Adv. Mater.* **2020**, *32*, 2001893. https://doi.org/10.1002/adma.202001893.
[4] S. Clair, D. G. De Oteyza, *Chem. Rev.* **2019**, *119*, 4717–4776. https://doi.org/10.1021/acs.chemrev.8b00601.
[5] Q. Shen, H.-Y. Gao, H. Fuchs, *Nano Today* **2017**, *13*, 77–96. https://doi.org/10.1016/j.nantod.2017.02.007.
[6] D. G. De Oteyza, T. Frederiksen, *J. Phys.: Condens. Matter* **2022**, *34*, 443001.
[7] M. C. Daugherty, P. H. Jacobse, J. Jiang, J. Jornet-Somoza, R. Dorit, Z. Wang, J. Lu, R. McCurdy, W. Tang, A. Rubio, S. G. Louie, M. F. Crommie, F. R. Fischer, *J. Am. Chem. Soc.* **2024**, *146*, 15879–15886. https://doi.org/10.1021/jacs.4c02386.
[8] N. Kocić, X. Liu, S. Chen, S. Decurtins, O. Krejčí, P. Jelínek, J. Repp, S.-X. Liu, *J. Am. Chem. Soc.* **2016**, *138*, 5585–5593.
[9] M. Bieri, M.-T. Nguyen, O. Gröning, J. Cai, M. Treier, K. Aït-Mansour, P. Ruffieux, C. A. Pignedoli, D. Passerone, M. Kastler, K. Müllen, R. Fasel, *J. Am. Chem. Soc.* **2010**, *132*, 16669–16676. https://doi.org/10.1021/ja107947z.
[10] N. Kalashnyk, E. Salomon, S. H. Mun, J. Jung, L. Giovanelli, T. Angot, F. Dumur, D. Gigmes, S. Clair, *ChemPhysChem* **2018**, *19*, 1802–1808. https://doi.org/10.1002/cphc.201800406.
[11] J. Dai, Q. Fan, T. Wang, J. Kuttner, G. Hilt, J. M. Gottfried, J. Zhu, *Phys. Chem. Chem. Phys.* **2016**, *18*, 20627–20634. https://doi.org/10.1039/C6CP03551E.
[12] S. Kawai, V. Haapasilta, B. D. Lindner, K. Tahara, P. Spijker, J. A. Buitendijk, R. Pawlak, T. Meier, Y. Tobe, A. S. Foster, E. Meyer, *Nat. Commun.* **2016**, *7*, 12711. https://doi.org/10.1038/ncomms12711.
[13] E. Pérez-Elvira, A. Barragán, Q. Chen, D. Soler-Polo, A. Sánchez-Grande, D. J. Vicent, K. Lauwaet, J. Santos, P. Mutombo, J. I. Mendieta-Moreno, B. De La Torre, J. M. Gallego, R. Miranda, N. Martín, P. Jelínek, J. I. Urgel, D. Écija, *Nat. Synth* **2023**, *2*, 1159–1170. https://doi.org/10.1038/s44160-023-00390-8.
[14] D. Peyrot, M. G. Silly, F. Silly, *J. Phys. Chem. C* **2017**, *121*, 26815–26821. https://doi.org/10.1021/acs.jpcc.7b08296.
[15] H. Klaasen, L. Liu, X. Meng, P. A. Held, H. Gao, D. Barton, C. Mück-Lichtenfeld, J. Neugebauer, H. Fuchs, A. Studer, *Chemistry A European J* **2018**, *24*, 15303–15308. https://doi.org/10.1002/chem.201802848.
[16] Z. Gong, B. Yang, H. Lin, Y. Tang, Z. Tang, J. Zhang, H. Zhang, Y. Li, Y. Xie, Q. Li, L. Chi, *ACS Nano* **2016**, *10*, 4228–4235. https://doi.org/10.1021/acsnano.5b07601.
[17] K. Biswas, J. Janeiro, A. Gallardo, M. Lozano, A. Barragán, B. Álvarez, D. Soler-Polo, O. Stetsovych, A. P. Solé, K. Lauwaet, J. M. Gallego, D. Pérez, R. Miranda, J. I. Urgel, P. Jelínek, D. Peña, D. Écija, *Nat. Synth* **2024**, *4*, 233–242. https://doi.org/10.1038/s44160-024-00665-8.
[18] B. Álvarez, J. Janeiro, A. Cobas, M. A. Ortuño, D. Peña, E. Guitián, D. Pérez, *Adv. Synth. Catal.* **2024**, *366*, 961–969. https://doi.org/10.1002/adsc.202301264.
[19] P. Hapala, G. Kichin, C. Wagner, F. S. Tautz, R. Temirov, P. Jelínek, *Phys. Rev. B* **2014**, *90*, 085421. https://doi.org/10.1103/PhysRevB.90.085421.
[20] O. Krejčí, P. Hapala, M. Ondráček, P. Jelínek, *Phys. Rev. B* **2017**, *95*, 045407.

Manuscript received: June 09, 2025
Revised manuscript received: August 27, 2025
Manuscript accepted: September 23, 2025
Version of record online: ■■, ■■

© 2025 The Author(s). Angewandte Chemie International Edition published by Wiley-VCH GmbH

15213773, 0, Downloaded from https://onlinelibrary.wiley.com/doi/10.1002/anie.202512575 by Universidad Autonoma De Madrid, Wiley Online Library on [30/10/2025]. See the Terms and Conditions (https://onlinelibrary.wiley.com/terms-and-conditions) on Wiley Online Library for rules of use; OA articles are governed by the applicable Creative Commons License